Int. J. Electrochem. Sci., 15 **(2020)** 8277 – 8283, doi: 10.20964/2020.08.41

International Journal of
ELECTROCHEMICAL
SCIENCE
www.electrochemsci.org

Short Communication

Imidazolate Framework (Zn-Ni(MeIm)$_2$) Nanohybrids as Electrodes for Supercapacitor Applications

Guoyong Xiao, Yinpeng Cao, Yunhua Lu, Haijun Chi, Zhizhi Hu[*], *Yue Wang*[*]

School of Chemical Engineering, University of Science and Technology Liaoning, 185 Qianshan Middle Road, Anshan, Liaoning, 114051, China
[*]E-mail: rosyue@163.com

Received: 28 March 2020 / *Accepted:* 7 May 2020 / *Published:* 10 July 2020

A typical solvothermal method was used to synthesize the imidazole framework (Zn-Ni(MeIm)$_2$) and subsequently calcined under a nitrogen atmosphere (Zn-Ni(MeIm)$_2$(N_2-723K), and activated with KOH (Zn-Ni(MeIm)$_2$(KOH)). The samples were characterized by X-ray diffraction, field emission scanning electron microscopy, Fourier transform infrared spectroscopy, and an electrochemical analyzer system. The pseudocapacitive behavior was exhibited when Zn-Ni(MeIm)$_2$ was used as a supercapacitor material in the electrolyte of 6 M KOH. The Zn-Ni(MeIm)$_2$, (Zn-Ni(MeIm)$_2$(N_2-723K) and (Zn-Ni(MeIm)$_2$(KOH) electrodes showed specific capacitances of 378, 192 and 573 Fg^{-1}, respectively, at a current density of 5 A g^{-1} . It still retained good performance and stability over 1000-cycles measurement. These results indicate that Zn-Ni(MeIm)$_2$-derived compounds are promising materials for use as supercapacitors.

Keywords: Imidazolate framework, Supercapacitors, Zn-Ni(MeIm)$_2$, Pseudocapacitance

1. INTRODUCTION

Supercapacitors are a new kind of electrochemical energy storage device with high power density, long cycle time and no pollution [1]. Electrode materials play an essential role in supercapacitors, which directly affects the energy storage of the device. Different forms of carbon have been used and applied for supercapacitor applications as electrode materials [2-4]. Details of the kinetics of ion diffusion through porous materials, as well as its importance in the use of nonaqueous electrolytes, were studied during recent decades [5-7]. In addition, high surface area, pore-size distribution [8-9], graphitic degree [10] and nitrogen content [11-12] have critical effects on obtaining a high-performance electric double-layer capacitor (EDLC). However, it is difficult to increase all the properties in supercapacitor's construction, which limits the development of supercapacitors. Thus, designed nanoporous carbon

(NPC) materials are synthesized and expected to significantly improve the electrochemical performance of current EDLC materials.

Supercapacitors have emerged as excellent candidates that can use as energy storage equipment due to their long life time, high power density, and minimal safety concerns [13]. Two types of supercapacitors have been developed: (1) electrochemical double layer capacitors (EDLCs), (2) pseudocapacitors. Usually, the electrostatically store charges at the surface of carbonaceous materials would lead to low specific capacitance, which limit the EDLCs application. Therefore, high-redox-active electrode compounds are promising materials with increasing interest. Pseudocapacitors are ideal alternative for better conductive materials which governed by multiple reversible faradic reactions during the charge and discharge processes [14].

Metal-organic frameworks (MOFs) are an increasingly developing class of porous materials. Due of their unique structural properties including high surface areas, tunable pore sizes, and open metal sites, MOFs have attracted great attention. The excellent characteristics of MOFs enable them to have potential applications in magnetism, gas storage, sensors, catalysis, and luminescence [15]. Herein, (Zn-Ni(MeIm)$_2$) was calcined under a nitrogen atmosphere, activated with KOH and subsequently investigated as an electrode material for supercapacitors with a 6 M KOH electrolyte. Zeolitic imidazolate frameworks (ZIFs) have the advantages of high stability and framework diversity [16]. ZIF-8 has excellent properties, including a large pore size and surface area, high thermal stability and good chemical stability [17]. Bimetallic MOFs with two different kinds of metal ions could improve the electrochemical characteristics [18]. To enhance the electrochemical performance of the prepared supercapacitor electrode, bimetal ions and ZIF were combined for the fabrication of the electrode material in this study. The preparation procedure is shown in Fig. 1. The results show that (Zn-Ni(MeIm)$_2$)(KOH) exhibits the best electrochemical performance.

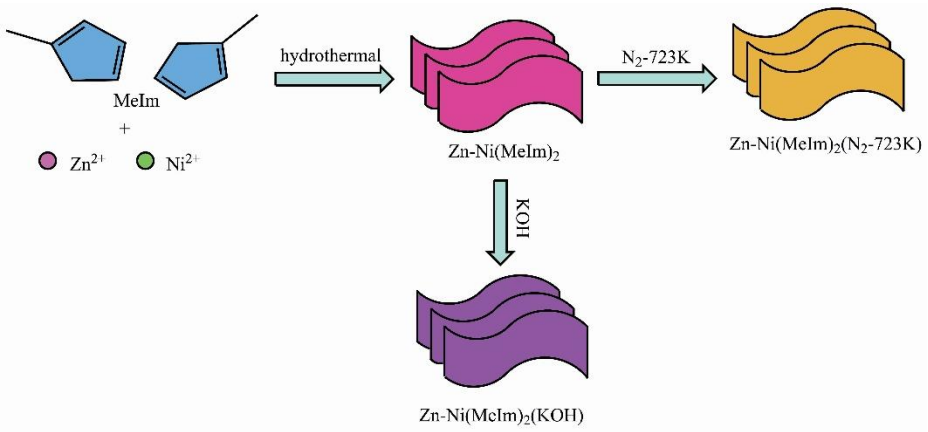

Figure 1. Preparation scheme of (Zn-Ni(MeIm)$_2$)-based materials

2. EXPERIMENTAL

2.1 Synthesis of the samples

The synthesis of Zn-Ni(MeIm)$_2$ was already reported [13]. Zinc nitrate hexahydrate ($ZnNO_3$•$6H_2O$, 1.189 g, 4.0 mmol), nickel(II) nitrate hexahydrate ($NiNO_2$•$6H_2O$, 1.163 g, 4.0 mmol)

and 2-methylimidaole (H-MeIm) (600 mg, 7.0 mmol) were mixed and dissolved in 40 mL of N,N-dimethylformamide (DMF) and 15 mL of ethylene glycol in a glass beaker. The mixture was stirred for 2 h at room temperature. Then, the mixture was transferred and sealed in a 100 mL autoclave and kept at 150 °C for 24 h. The received material (Zn-Ni(MeIm)$_2$) was filtered and then washed with ethanol and DMF separately. The material was dried overnight after cooling down. Then, Zn-Ni(MeIm)$_2$ was calcined under a nitrogen atmosphere at 723 K for 3 h, and the product was denoted as (Zn-Ni(MeIm)$_2$(N_2-723K). Zn-Ni(MeIm)$_2$ was then immersed in 2 M KOH with stirring at room temperature for 5 h. Furthermore, the solid was washed by deionized water to remove the redundant KOH. Finally, Zn-Ni(MeIm)$_2$ (KOH) was obtained after drying in an oven overnight.

2.2 Characterization

A Nicolet is10 Fourier transform infrared (FTIR) spectrophotometer was used to characterize the chemical structures of the prepared materials, scanning from 600 to 4000 cm^{-1}. The crystallographic data were measured by using an X'Pert Powder X-ray diffractometer (PANalytical, Netherlands). The X-ray diffraction (XRD) pattern was measured from 5° to 50° (2θ value) with Cu$K\alpha$ radiation (conditions: λ= 1.54 Å, 40 kV, 40 mA). Field emission scanning electron microscopy (FE-SEM) images were collected with a Zeiss-IGMA HD field emission scanning electron microscope (Germany) at a working voltage of 2.0 kV. The electrodes were prepared by pressing at pastes of 75: 20: 5 wt% active material/carbon black/polytetrafluoroethylene (PTFE) at a pressure of 10 MPa. The prepared electrode was dried at 100 °C for 2 h. Nickel foam was used as the current collector. Electrochemical measurements were carried out on an IVIUM (Holland) electrochemical analysis system in a three-electrode system. The active material powder worked as the working electrode, with an Ag/AgCl electrode as the reference electrode [19], and a platinum sheet electrode as the counter electrode. The electrode was prepared by 6 M of KOH. Cyclic voltammetry (CVs) was used to carry out the check scan rates tendency within a potential range. Galvanostatic charge–discharge (GCD) was conducted at a current density of 1 A g^{-1}. The chronopotentiometry test was carried out within a potential window.

3. RESULTS AND DISCUSSION

3.1 Physicochemical characterization

The XRD patterns of the synthesized compounds are shown in Fig. 2a. The results indicate that in comparison to the reported Zn(MeIm)$_2$ structure [17], the prepared compounds contain Zn(MeIm)$_2$. Zn-Ni(MeIm)$_2$ is highly crystalline, as we can see from the sharp peaks in the XRD patterns. The slight difference in XRD patterns may be caused by the metastable state of semicrystalline to crystalline [20]. It may disappear with a change in external conditions and transform into a stable crystalline state, eventually forming Zn-Ni(MeIm)$_2$ with complete crystallinity. The crystalline order of Zn-Ni(MeIm)$_2$ remains mostly unchanged after being calcined under a nitrogen atmosphere at 723 K. The FT-IR spectrum in Fig. 2b shows that the adsorption peak at 1666 cm^{-1} almost disappeared after calcination of

Zn-Ni(MeIm)$_2$ under a nitrogen atmosphere and KOH treatment. This indicates that the guest molecules (DMF and H_2O) are removed or carbonized.

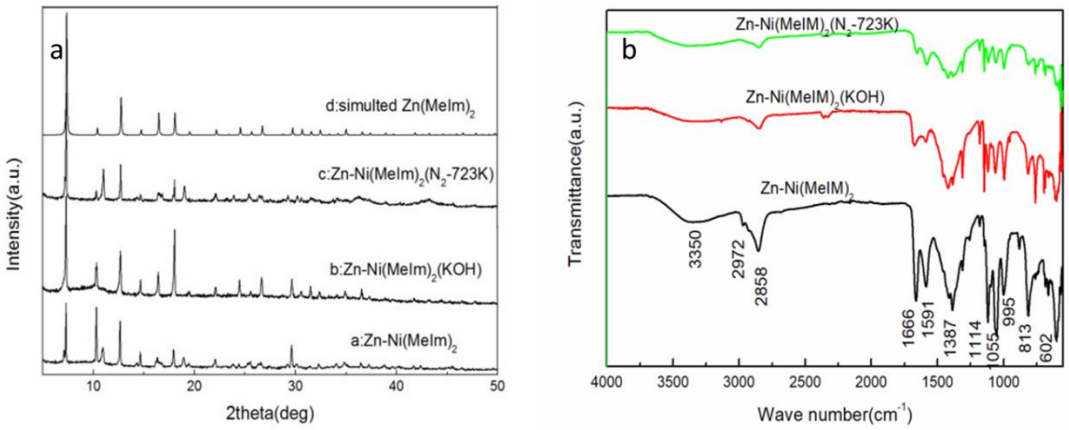

Figure 2. XRD patterns (a) and FT-IR spectra (b) of the synthesized compounds.

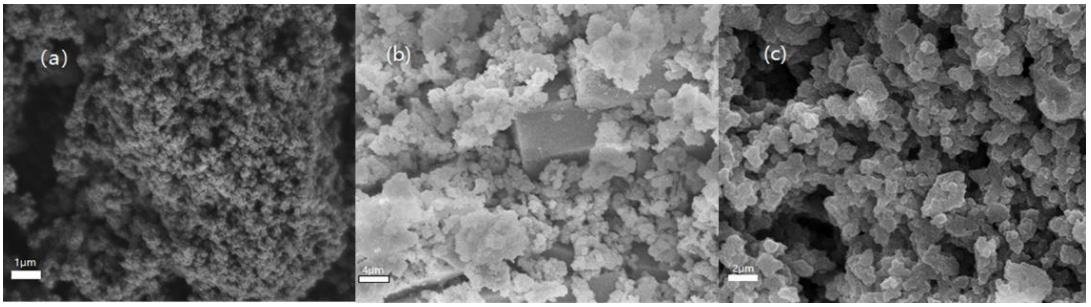

Figure 3. FE-SEM images of (a) Zn-Ni(MeIm)$_2$, (b) (Zn-Ni(MeIm)$_2$(N$_2$-723K), and (c) (Zn-Ni(MeIm)$_2$(KOH).

The SEM images of the as-prepared samples are presented in Fig. 3. Fig. 3a shows a high-porosity structure composed of spherical-like nanoscale particles. However, after carbonization at 723 K, some of the pore structures collapsed (in Fig. 3b). As shown in Fig. 3c, the pores became more abundant after activation by KOH, which would accelerate electron transfer rate for electrolyte to penetrate to the inner of the electrode material.

3.2 Electrochemical properties

Fig. 4a-c show the CV curves for the untreated Zn-Ni(MeIm)$_2$, the calcined Zn-Ni(MeIm)$_2$ under a nitrogen atmosphere, and Zn-Ni(MeIm)$_2$ after KOH treatment, respectively, at different scan rates. The CVs were measured at a scan rate of 5 mVs^{-1} on different sample electrodes and are shown in Fig. 4d. Judging from the CV curves, the reaction is a quasi-reversible electron transfer process. The results indicating that the capacitance is based on a redox mechanism [21], which is different from that of EDLCs. The CV curve for EDLCs is close to an ideal rectangular shape. The anodic peak of the

electrodes shifts positively with increasing scan rate, while the cathodic peaks shift negatively. The specific capacitance (Cs) can be estimated using the following well-known formula [22].

$$Cs=(I \times \Delta t)/(m \times \Delta V) \quad (1)$$

where the specific capacitance is simplified as Cs (Fg^{-1}) and the discharge current and time are symbolized as I(A) and Δt(s), respectively. The potential window and mass of a single electrode are expressed by ΔV(V) and m(g), respectively.

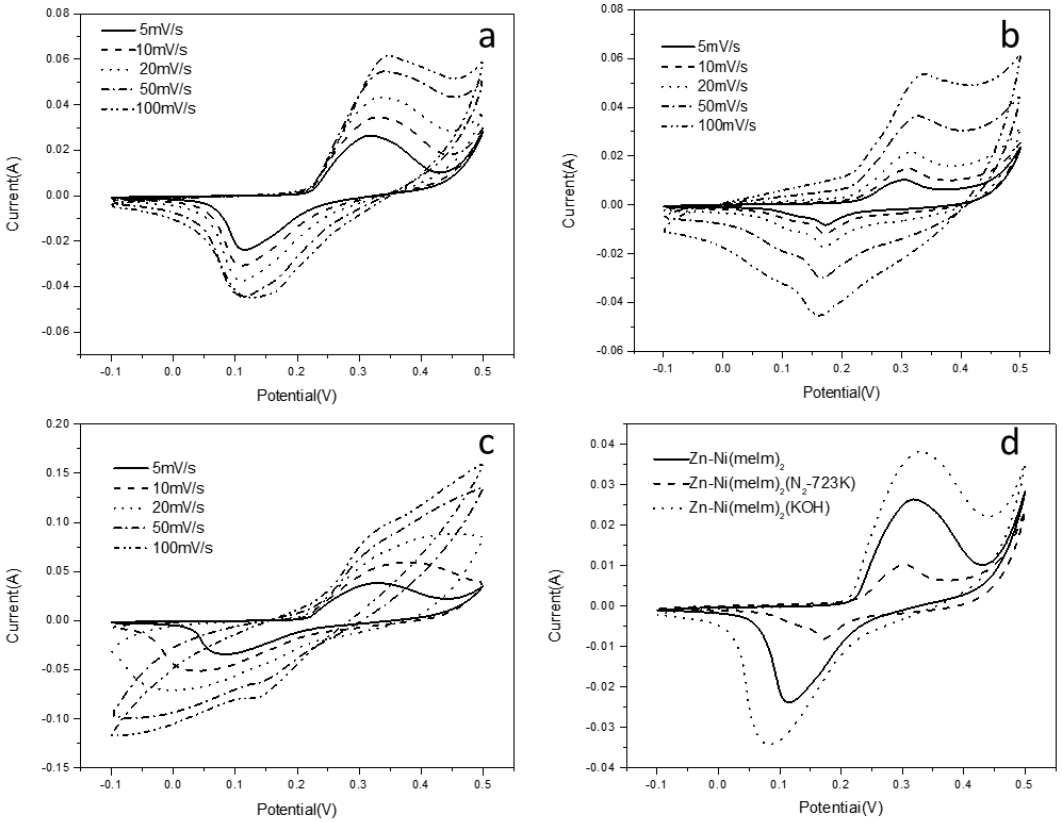

Figure 4. CV curves of different samples at various scanning rates. a Zn-Ni(MeIm)$_2$. b Zn-Ni(MeIm)$_2$ (N_2-723K). c Zn-Ni(MeIm)$_2$(KOH). d CV curves of different samples with a scan rate of 5 mVs^{-1}

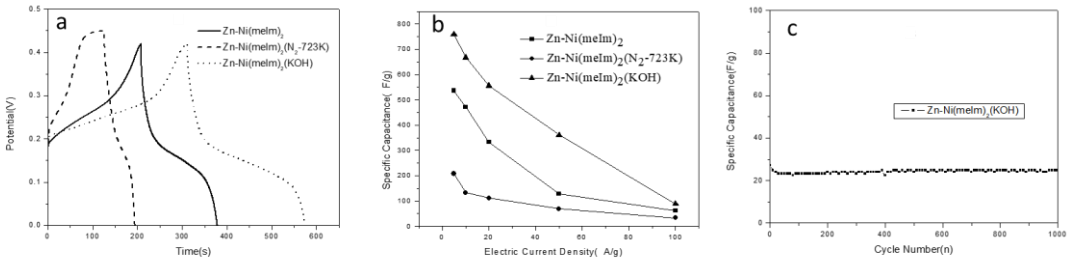

Figure 5. a, GCD curves of different samples at a current density of 1 A g^{-1}. b, The specific capacitance of different samples at different current densities. c, Cycling performance of experimental Zn-Ni(MeIm)$_2$ (KOH) at a current density of 5 A g^{-1}.

The GCD curves of Zn-Ni(MeIm)$_2$, Zn-Ni(MeIm)$_2$ (N_2-723K) and Zn-Ni(MeIm)$_2$ (KOH) at 1 A g^{-1} are plotted in Fig. 5a for comparison. The specific capacitances are 378, 192 and 573 F g^{-1} for Zn-Ni(MeIm)$_2$, Zn-Ni(MeIm)$_2$ (N_2-723K) and Zn-Ni(MeIm)$_2$ (KOH), respectively, based on eq. (1). The calculated specific capacitance at various current densities of Zn-Ni(MeIm)$_2$, Zn-Ni(MeIm)$_2$ (N_2-723K) and Zn-Ni(MeIm)$_2$ (KOH) according to eq. (1) is exhibited in Fig. 5b. Clearly, Zn-Ni(MeIm)$_2$ (KOH) delivers a higher specific capacitance than Zn-Ni(MeIm)$_2$ (378 F g^{-1}) and Zn-Ni(MeIm)$_2$ (N_2-723K) (192 F g^{-1}). Zn-Ni(MeIm)$_2$ (KOH) could reach a value of 573 F g^{-1} even when the current density was increased to 1 A g^{-1}, indicating faster electron transfer in the Zn-Ni(MeIm)$_2$ (KOH) electrode. These findings verify that Zn-Ni(MeIm)$_2$ (KOH) has satisfactory rate capability and higher specific capacitance than Zn-Ni(MeIm)$_2$.

Table 1. Summary of typical MOF-based supercapacitor electrode materials.

Electrode	Capacitance (F g^{-1})	Current density (A g^{-1})	Ref
$[CuIH_2(C_{12}H_{12}N_6)(PMo_{12}O_{40})]\cdot(C_6H_{15}N)[(H_2O)_2]$	239.2	3	23
Ni/Co-MOFs	1220.2	1	24
Eu-MOF	468	1	25
Co_3O_4	342.1	0.5	26
(Zn-Ni(MeIm)$_2$	573	5	This work

As shown in Fig. 5c, the stability of the Zn-Ni(MeIm)$_2$ (KOH) electrode was examined through CV cycle life tests carried out at a current density of 5 A g^{-1}. The results showed that the specific capacitance of the electrode continuously increases until 1000 cycles. That indicated the full activation at the electrode/electrolyte interface, and the value of the specific capacitance is almost constant. Moreover, the specific capacitance of MOF-based supercapacitor materials is summarized in Table 1. Compared to that of previously reported materials, the performance of the materials described herein is acceptable. These results suggest that Zn-Ni(MeIm)$_2$ (KOH) is a very suitable and valuable electrode material for supercapacitors.

4. CONCLUSION

In this study, Zn-Ni(MeIm)$_2$ was calcined and/or treated with KOH and then evaluated as an electrode material for supercapacitor in a KOH electrolyte. The cyclic voltammetry and chronopotentiometry measurements indicate that the capacitance of Zn-Ni(MeIm)$_2$ mainly caused by Faradaic reactions. Zn-Ni(MeIm)$_2$ (KOH) shows a maximum specific capacitance value of 573 F g^{-1} even when the current density is increased to 1 A g^{-1}. This Bimetallic MOFs based electrode material is a promising material for the future application in supercapacitor devices.

ACKNOWLEDGMENT
This study was financially supported by the Natural Science Foundation of Liaoning Province (No. 20180550439) and the Talent Project of Liaoning University of Science and Technology (No. 601011507-17).

References

1. F. Bonaccorso, L. Colombo, G. Yu, M. Stoller, V. Tozzini, A.C. Ferrai, R. S. Ruoff and V. Pellegrini, *Science*, 347 (2015) 1246501.
2. P. Simon and Y. Gogotsi, *Acc. Chem. Res.*, 46 (2013) 1094.
3. M. Kaempgen, C. K. Chan, J. Ma, Y. Cui and G. Gruner, *NanoLett.*, 9 (2009) 1872.
4. H. Jiang, P. S. Lee and C. Li, *Energy Environ. Sci.*, 6 (2013) 41.
5. J. Chmiola, G. Yushin, Y. Gogotsi, C. Portet, P. Simon and P. L.Taberna, *Science*, 313 (2006) 1760.
6. D. E. Jiang, Z. Jin, D. Henderson and J. Wu, *J. Phys. Chem. Lett.*, 3 (2012) 1727.
7. J. Huang, B. G. Sumpter and V. Meunier, *Chem. Eur. J.*, 14 (2008) 6614.
8. J. Chmiola, G. Yushin, R. Dash and Y. Gogotsi, *J. Power Sources*, 158 (2006) 765.
9. G. Gryglewicz, J. Machniko wski, E. Lorenc-Grabowska, G. Lota and E. Frack owiak, *Electrochim. Acta*, 50 (2005) 1197.
10. N. L. Torad, R. R. Salunkhe, Y. Li, H. Hamoudi, M. Imura, Y. Sakka, C. C. Hu and Y. Yamauchi, *Chem. Eur. J.*, , 20 (2014) 7895.
11. D. Hulicova, M. Kodama and H. Hatori, *Chem.Mater.*, 18 (2006) 2318.
12. R. R. Salunkhe, Y. H. Lee, K. H. Chang, J.M. Li, P. Simon, J. Tang,N. L. Torad, C. C. Hu and Y. Yamauchi, *Chem. -Eur. J.*, 20 (2014) 13838.
13. G. Fu, L. Ma, M. Gan, X. Zhang, M. Jin, Y. Lei, P. Yang and M. Yan, *Synth. Met.*, 224 (2017) 36.
14. M. Shao, F. Ning, Y. Zhao, J. Zhao, M. Wei, D.G. Evans and X. Duan, *Chem. Mater.*, 24 (2012) 1192.
15. G. Lu and J.T. Hupp, *J. Am. Chem. Soc.*, 132 (2010) 7832.
16. Y. Gao, J. Wu, W. Zhang, Y. Tan, J. Gao, J. Zhao and B. Tang, *J Solid State Electrochem.*, 18 (2014) 3203.
17. K. S. Park, Z. Ni, A. P. Cote, J. Y. Choi, R. D. Huang, F. J. Uribe-Romo, H. K. Chae, M. O'Keeffe and O. M. Yaghi, Proc. Natl. Acad. Sci. U.S.A. 103 (2006) 10186.
18. J. Yang, C. Zheng, P. Xiong, Y. Li and M. Wei, *J. Mater. Chem. A*, 2 (2014) 19005.
19. R. Diaz, M.G. Orcajo, J. A. Botas, G. Calleja and J. palma, *Mater. Lett.*, 68 (2012) 126.
20. S. R. Venna, J. B. Jasinkki and M.A. Crreon, *J. Am. Chem. Soc.*, 132 (2010) 18030.
21. P. Oliva, J. Leonardi, J. F. Laurent, C. Delmas, J. J. Braconnier, M. Figlarz, F. Fievet and A. Guibert, *J. Power Sources*, 8 (1982) 229.
22. X. Zhang, L. Ma, M. Gan, G. Fu, M. jin, Y. Lei and P. Yang, *J. Power Sources*, 340 (2017) 22.
23. D. Chai, J. Xin, B. Li, H. Pang, H. Ma, K. Li, B. Xiao, X. Wang and L. Tan, Dalton Trans., 48 (2019) 13017.
24. C. Chen, M. Wu, K. Tao, J. Zhou, Y. Li, X. Han and L. Han, Dalton Trans., 47 (2018) 5639.
25. A. S. Dezfuli, E. Kohan, H. R. Naderi and E. Salehi, New J. Chem., 43 (2019) 9260.
26. Z. Zhu, C. Han, T.-T. Li, Y. Hu, J. Qian, S. Huang, *CrystEngComm*, 27 (2018) 3812